New Insights into Applicability of Electron-Counting Rules in Transition Metal Encapsulating Ge Cage Clusters

ARTICLE *in* THE JOURNAL OF PHYSICAL CHEMISTRY A · DECEMBER 2010

Impact Factor: 2.69 · DOI: 10.1021/jp106354d · Source: PubMed

3 AUTHORS, INCLUDING:

Debashis Bandyopadhyay
Birla Institute of Technology and Science P…
49 PUBLICATIONS **239** CITATIONS
SEE PROFILE

Prasenjit Sen
Harish-Chandra Research Institute
61 PUBLICATIONS **675** CITATIONS
SEE PROFILE

New Insights into Applicability of Electron-Counting Rules in Transition Metal Encapsulating Ge Cage Clusters

Debashis Bandyopadhyay,[†] Prabhsharan Kaur,[‡] and Prasenjit Sen*[,§]

Physics Group, Birla Institute of Technology and Science, Pilani, Rajasthan, India, Physics Department, National Institute of Technology, Hamirpur, HP, India, and Harish-Chandra Research Institute, Chhatnag Road, Jhunsi, Allahabad 211019, India

Received: July 9, 2010; Revised Manuscript Received: October 28, 2010

The relative stability of Sc, Ti, and V encapsulating Ge_n clusters in the size range $n = 14-20$ has been studied through first-principles electronic structure calculations based on density functional theory. Variations of the embedding energy, gap between the highest occupied and the lowest occupied molecular orbitals, ionization potential, vertical detachment energy, and electron affinity with cluster size have been calculated to identify clusters with enhanced stability. The enhanced stability of some clusters can be very well explained as due to the formation of a filled shell free-electron gas inside the Ge cages. For the first time, direct evidence of the formation of a free-electron gas is also presented. In some other clusters, enhanced stability is found to originate from geometric effects. Some clusters that may be expected to have enhanced stability from simple electron counting rules do not show that. These results provide new insights into the long-standing question of whether electron counting rules can explain the relative stability of transition metal encapsulated semiconductor clusters and show that these clusters are too complex for such simple generalizations.

1. Introduction

Production of transition metal (TM) doped Si clusters by Hiura et al.[1] generated a lot of interest and a flurry of activities on TM encapsulated semiconductor clusters.[2−19] While the initial excitement is over, some of the outstanding questions still remain unanswered. One of the major findings of Hiura et al.[1] was that among the 5d TM doped Si clusters, WSi_{12} was the most stable. An attempt was made to explain this in terms of the octet rule borrowed from organometallic chemistry. This rule claims that when the total number of valence electrons on a TM atom surrounded by other atoms or ligands is 18, the molecule or ion is particularly stable. Assuming that each Si atom donates one valence electron to the encapsulated TM atom, the total valence electron count on the latter in a $TMSi_n$ is $n + n_M$, when n_M is the number of valence electrons on the TM atom. By this argument, WSi_{12} (with $n_M = 6$) should be the most stable cluster in the 5d TM doped Si_{12} series. Similarly, $CrSi_{12}$ should be most stable among the 3d TM doped Si_{12} clusters. There was a debate in the literature whether this electron-counting rule is valid in TM-Si clusters. Sen and Mitas[17] and Guo et al.[9] in their calculations found VSi_{12} to be the most stable cluster in the 3d series, as indicated by their embedding energies (EE). It was claimed that the octet rule is not always valid. Reveles and Khanna,[18] based on their density functional theory (DFT) calculations, invoked different electron-counting rules to explain the enhanced stability of TM-Si clusters. They argued that (a) valence electrons in TM-Si clusters form a nearly free-electron gas and (b) one needs to invoke the Wigner−Witmer (WW) spin conservation rule[20] while calculating the EE. Imposing the WW rule, they showed that $CrSi_{12}$, indeed, has the highest EE in the neutral 3d TM doped Si_{12} clusters. Ignoring the WW rule was claimed to be the reason why VSi_{12} turned out to have the highest EE. In the nearly free-electron gas picture, the metal atom is assumed to donate all of its valence electrons, and each Si atom is assumed to donate one electron to the valence pool. Alongside the major peak at $CrSi_{12}$, Reveles and Khanna[18] found a smaller peak in EE at $FeSi_{12}$, which can be justified as originating from a 20-electron filled shell electronic configuration. Among the anionic clusters, VSi_{12}^- has the highest EE, being an 18-electron cluster. It is worth mentioning here that the one-electron levels in spherically confined free-electron gas follow the sequence $1S^21P^61D^{10}2S^2...$[21] Thus, 2, 8, 18, 20, etc. are the shell-filling numbers, and clusters having these numbers of valence electrons attain enhanced stability. However, the free-electron gas picture was apparently violated in some TM-Si clusters.[18] There is no peak in EE at $MnSi_{12}^-$, which is a 20-electron cluster. Moreover, there is a small peak at $CoSi_{12}^-$, which is a 22-electron cluster. On the other hand, experiments have supported the validity of these electron-counting rules in some cases. Koyasu et al.[7] studied the electronic and geometric structures of $TMSi_{16}$ (TM = Sc, Ti, and V) clusters by mass spectrometry and anion photoelectron spectroscopy. They found that neutral $TiSi_{16}$, being a 20-electron cluster, has a closed-shell electron configuration with a large gap between the highest occupied and the lowest unoccupied molecular orbitals (HOMO−LUMO gap). $ScSi_{16}$ anions and VSi_{16} cations, both being 20-electron clusters, were also produced in greater abundance.

TM-Si clusters having been explored in some detail, recently, there has been a focus on TM-Ge clusters.[22−24] It has been shown by us[24] and other workers[22] that among the Ni encapsulating neutral and cation clusters, $NiGe_{10}$ and $NiGe_{11}^+$, both having 20 valence electrons, are the most stable ones. In our calculations, these two clusters were found to have peaks in EE, second order energy difference, and HOMO−LUMO gap. Also, interesting was the finding that the ionization potential (IP) of

* To whom correspondence should be addressed. E-mail: prasen@hri.res.in.
[†] Birla Institute of Technology and Science.
[‡] National Institute of Technology.
[§] Harish-Chandra Research Institute.

10.1021/jp106354d
Published on Web 11/23/2010

$NiGe_n$ clusters drops sharply from $n = 10$ to 11, indicating enhanced stability of $NiGe_{10}$ due to shell filling.

Although the enhanced stability of WSi_{12}, $CrSi_{12}$, VSi_{12}^-, $FeSi_{12}$, $NiGe_{10}$, and $NiGe_{11}^+$ clusters indicates the existence of electronic shells, whether a nearly free-electron gas is formed in TM doped Si or Ge clusters deserves closer attention. Reveles and Khanna[18] addressed this question to some extent. In $FeSi_{12}$, a 20-electron cluster, they found a doubly occupied HOMO akin to the 2S state. In $CrSi_{12}$, an 18-electron cluster, they found a bunch of nearly degenerate HOMO levels, as expected for d-like states. They also found that $ScSi_{16}$ anions, $TiSi_{16}$ and VSi_{16} cations are the most stable among Sc, Ti, and V encapsulating Si clusters in the size range that they studied,[19] in agreement with Koyasu et al.'s[7] experiments. These were explained as originating from 20-electron filled shell configurations. A simple-minded electron count would suggest that $ScSi_{17}$ and $TiSi_{17}^+$ are also 20-electron clusters. However, these are not found in great abundance in experiments.[7] Reveles and Khanna[19] argued that a Si atom donates an electron to the nearly free-electron gas only if it forms a bond with the TM atom. This analysis showed that $ScSi_{17}$ and $TiSi_{17}^+$ are not 20-electron clusters. However, this analysis also does not give a direct answer to the question if there is, indeed, a free-electron gas in TM-Si clusters.

Coming back to the case of TM-Ge clusters, while the enhanced stability of 20-electron $NiGe_{10}$ cluster was established, no further exploration of the free-electron gas has yet been done. In this paper, we explore deeper into the issue of the formation of free-electron gas inside the TM encapsulating Ge cage. For this, we study the relative stability of Sc, Ti, and V encapsulating Ge_n clusters in the size range $n = 14-20$. We identify clusters with enhanced stability by peaks in their EE and HOMO−LUMO gap when plotted as a function of cluster size, that is, the number of Ge atoms, and also through features in vertical detachment energy (VDE) and electron affinity (EA) as discussed below. Peaks in EE and HOMO−LUMO gap are indications of thermodynamic and kinetic stability, respectively. The WW spin conservation rule is imposed while calculating EE. EE is the energy gain in incorporating a TM atom in the lowest energy isomer of the pure Ge_n cluster. In the case of a neutral cluster, this is defined as

$$\mathrm{EE} = E_\mathrm{T}(\mathrm{Ge}_n) + E_\mathrm{T}(\mathrm{TM}) - E_\mathrm{T}(\mathrm{TMGe}_n) \qquad (1)$$

E_T values are the total energies. In case the ground state multiplicities of the respective systems do not conserve total spin, the energy of the TM atom in an appropriate spin excited state was taken to enforce the WW spin conservation rule. For charged clusters, there are two possibilities,

$$\mathrm{EE} = E_\mathrm{T}(\mathrm{Ge}_n^{\pm}) + E_\mathrm{T}(\mathrm{TM}) - E_\mathrm{T}(\mathrm{TMGe}_n) \qquad (2a)$$

or

$$\mathrm{EE} = E_\mathrm{T}(\mathrm{Ge}_n) + E_\mathrm{T}(\mathrm{TM}^{\pm}) - E_\mathrm{T}(\mathrm{TMGe}_n) \qquad (2b)$$

either the charged TM atom can be embedded in a neutral Ge_n cluster or the other way round. We take the lower of these two numbers as the EE with enforcement of the WW spin conservation rule.

We use the topological features of the molecular electrostatic potential (MEP) to identify TM-Ge bonds and to visualize if there is a region of enhanced electron density around the TM atom inside the Ge cages. Use of topological features of various molecular scalar fields to describe bond formation between pairs of atoms, or other properties of a molecule, was introduced by Bader and other researchers.[25,26] Electron charge density, Laplacian of the electron charge density, the elctron localization function, and the MEP have all been used in different contexts. MEP, which is simply the electrostatic potential felt by a test unit positive charge at a point in space, has certain advantages over other scalar fields.[26] In particular, MEP shows minima in electron-rich regions such as for lone pairs and π electrons, as shown in ref 26. This is absent for electronic charge density. This prompts use of MEP to track electron-rich region in these clusters. The topological feature of MEP relevant here is its critical points (CPs), points where its gradient vanishes. Eigenvalues of the Hessian matrix of the MEP at such CPs carry necessary information about bonding, electron delocalization, etc. A CP is characterized as (R,S). Rank R of a CP is the number of nonzero eigenvalues of the Hessian matrix that that CP, and signature S is the algebraic sum of the signs of the eigenvalues. Clearly, no CP can have rank greater than 3, and for CPs of rank 3, the possible values of S are -3, -1, $+1$, and $+3$. Existence of $(3, -1)$ CPs in the MEP is taken as an indication of bond formation between a pair of atoms, and these are called bond CPs. $(3, +3)$ CPs mark local minima in the MEP. Clearly, there are a large number of bonds between various pairs of atoms. For our purposes, we report only the bonds between the TM atom and the Ge atoms. Electron-rich regions should have local minima in the MEP marked by $(3, +3)$ CPs, and we track such CPs only within the Ge_n cage. The complete topology of the MEP of these clusters is quite complicated, and there are a large number of $(3, +1)$ and $(3, -3)$ CPs also, which we ignore.

2. Computational Methods

Self-consistent field (SCF) electronic structure calculations are carried out on all clusters within the framework of Kohn−Sham DFT. Molecular orbitals (MOs) are expressed as a linear combination of atom-centered basis functions for which the LanL2DZ (5D, 7F) basis sets, and associated effective core potential (ECP), are used on all atoms. Spin-polarized calculations are carried out using the Becke three-parameter exchange and the Perdew−Wang generalized gradient approximation (GGA) (B3PW91) functional.[27,28] For all clusters, geometries were optimized without any symmetry constraints starting from a number of initial configurations and for different spin states. The stability of the structures is checked by calculating their harmonic vibrational frequencies. If any imaginary frequency is found, further relaxation is carried out until the true local minimum is obtained. Total energy and harmonic frequency for all of the clusters are calculated using the GAUSSIAN03 program package.[29] CPs of the MEP are then located for a select set of clusters using the deMon2K[30] code. The same basis sets and ECPs as in GAUSSIAN03, and PW86 GGA exchange-correlation functional are used in these calculations.

3. Results and Discussion

On the basis of our previous work[24,31] on TM doped Ge and Si clusters, a number of initial structures for Ge cages encapsulating TM atoms are formed at each size. These are then optimized as stated earlier. Structures with the TM atom outside the Ge cage have also been tried in some cases. These always turn out to have higher energies. Optimized ground state structures for select clusters along with the relevant $(3, -1)$

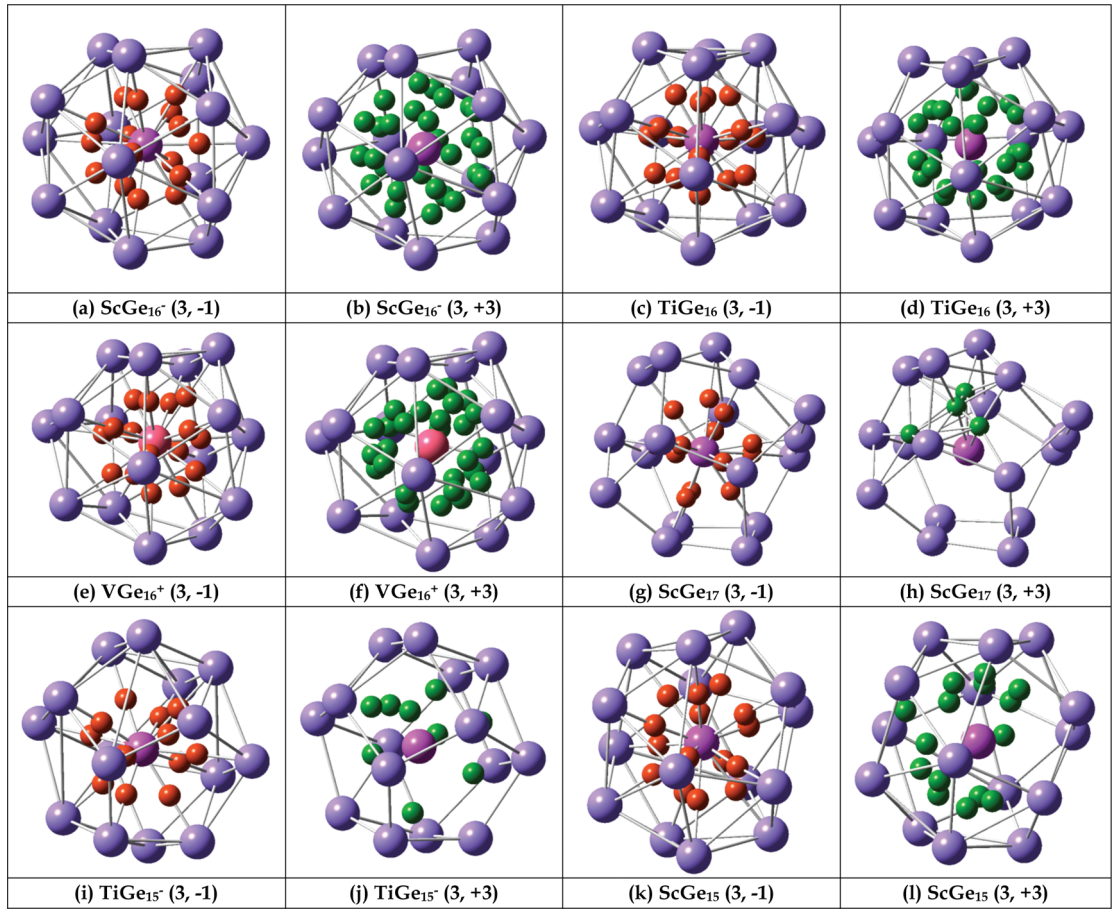

Figure 1. Structures and locations of (3, −1) and (3, +3) CPs for select $TMGe_n$ clusters. Purple and pink (larger) balls represent the Ge and TM (at the center of each cage) atoms. Red and green (smaller) balls represent the (3, −1) and (3, +1) CPs, respectively, as marked below each panel.

and (3, +3) CPs are shown in Figure 1 and Figure S1 in the Supporting Information. Details of the structures can be found elsewhere.[24]

The main focus of the work is to study the relative stability of Sc, Ti, and V encapsulating Ge_n clusters in neutral and singly ionized positive and negative charge states and to explore how far any enhanced stability can be explained by the formation of a closed shell free-electron gas inside the Ge cages. For the first time, we ask if an electron-rich region spread uniformly around the TM atom can be unequivocally identified and visualized. By a naive electron counting, where one assumes that each Ge atom in the cluster donates one electron to the free-electron gas, one should find several 18-electron and 20-electron clusters in the above range. These are as follows. The possible 18-electron clusters are $ScGe_{15}$, $ScGe_{16}^+$, and $TiGe_{15}^+$, and the possible 20-electron clusters are $ScGe_{17}$, $ScGe_{16}^-$, $ScGe_{18}^+$, $TiGe_{16}$, $TiGe_{15}^-$, $TiGe_{17}^+$, VGe_{15}, and VGe_{16}^+. This list excludes clusters having 14 Ge atoms. Being the first in the series, it is not possible to determine if they have peaks in EE or HOMO−LUMO gap. However, this will not affect our major conclusions, as will become clear later. The questions we pose are as follows: Do all of these clusters, indeed, show enhanced stability? If and how far can the observations be rationalized in terms of electron-counting rules? Also, can one find a direct evidence of formation of an electron gas inside the Ge cage encapsulating TM atoms?

Figure 2 shows the EEs of Sc, Ti, and V encapsulated Ge_n neutral, cation, and anion clusters as a function of cluster size n. It is clear that $ScGe_{16}^-$ has the highest EE among the Sc encapsulated clusters. Among the Ti encapsulated clusters, $TiGe_{15}^-$ has the highest EE, and those of $TiGe_{15}^+$ and $TiGe_{16}$ are very close. VGe_{16}^+ and VGe_{18}^+ have the highest EEs among the V encapsulated clusters, the values being within 0.01 eV. Figure 3 shows the HOMO−LUMO gaps of these clusters. Again, it is clear that among the Sc, Ti, and V encapsulated clusters, $ScGe_{16}^-$, $TiGe_{16}$, and VGe_{16}^+ have the highest HOMO−LUMO gaps. Thus, both of these quantities indicate enhanced stability of the $ScGe_{16}^-$, $TiGe_{16}$, and VGe_{16}^+ clusters. We now analyze the stability of these clusters from their electronic structure.

As already mentioned in the context of TM encapsulating Si clusters, $ScSi_{16}^-$, $TiSi_{16}$, and VSi_{16}^+ were found to be the most stable ones due to formation of a filled shell free-electron gas inside the Si cage.[7,19] It is likely that the same mechanism leads to the enhanced stability of the $ScGe_{16}^-$, $TiGe_{16}$, and VGe_{16}^+ clusters. Before we go on to analyze that, we also monitor the variation of EE of the Sc, Ti, and V encapsulated Ge_{16} clusters with their charge state. As shown in Figure 4, the Sc, Ti, and V encapsulated Ge_{16} clusters have the highest EE in the anion, neutral, and cation states, respectively, indicating enhanced stability of these clusters. Now, to address the question if a free-electron gas forms inside the Ge_{16} cage in these clusters, we located the (3, +3) CPs inside the cage. These are shown in Figure 1b,d,f. It is clearly seen that in all of these clusters, there is a large number of (3, +3) CPs inside the Ge_{16} cage almost uniformly surrounding the encapsulated TM atoms. This is perhaps the first direct evidence of formation of a uniform electron-rich region due to delocalized electrons inside the cage. The (3, −1) CPs are also shown in Figure 1a,c,e. Locations of the (3, −1) CPs, indicate that all of the 16 Ge atoms form bonds

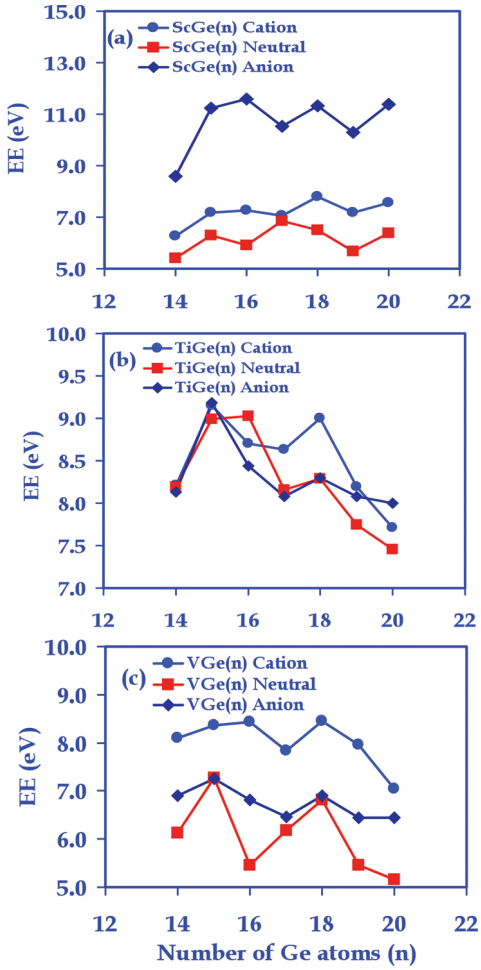

Figure 2. EEs of (a) Sc, (b) Ti, and (c) V encapsulating Ge_n clusters. EEs for neutral and singly ionized anion and cation clusters have been shown.

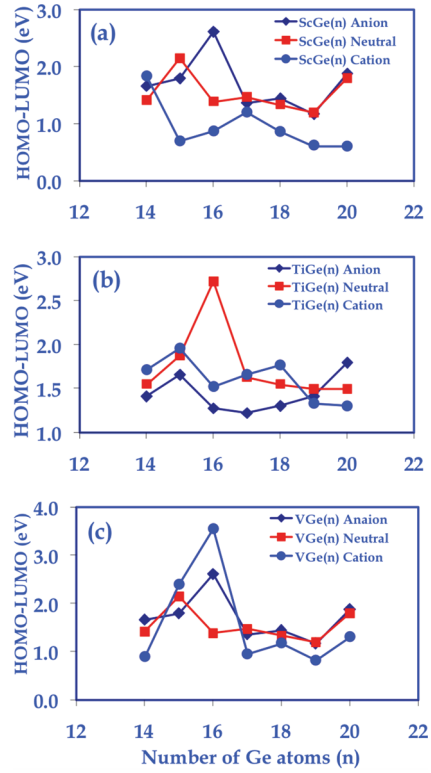

Figure 3. HOMO−LUMO gaps of (a) Sc, (b) Ti, and (c) V encapsulating Ge_n clusters. Gaps of neutral and singly ionized anion and cation clusters have been shown.

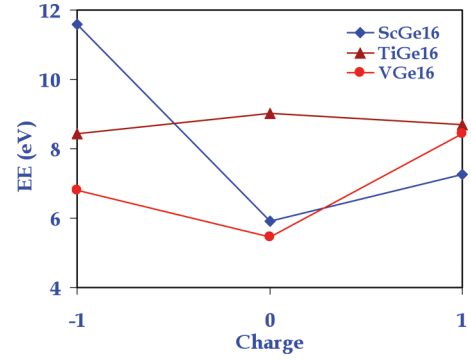

Figure 4. Variation of EE of Sc, Ti, and V encapsulating Ge_{16} clusters with their charge state.

with the TM atoms in these clusters. If each Ge atom bonded to the TM atom is assumed to donate one electron, all of these clusters have 20 valence electrons. Thus, not only do the electron-counting rules originating from a free-electron gas picture explain the enhanced stability of the $ScGe_{16}^-$, $TiGe_{16}$, and VGe_{16}^+ clusters, but they also derive justification for their applicability from a direct evidence of formation of a nearly uniform electron-rich region inside the Ge cage.

We also posed the question if the one-electron levels in these clusters correspond to the levels in spherically confined free-electron gas. In such a scenario, a 20-electron cluster should have a single nondegenerate HOMO corresponding to the 2S level. $ScGe_{16}$, $TiGe_{16}$, and VGe_{16}^+ all have nearly 5-fold degenerate HOMO. The MOs lower than the top five are bunched differently in the three clusters without any obvious correspondence to the levels in a spherical free-electron gas. Also, the angular character of some of the top five occupied levels cannot be identified with 1D states of a free-electron gas. In particular, although the major contribution to these MOs is from the TM d orbitals, the Ge orbitals also contribute substantially, making their resulting shapes quite different from d orbitals in many cases. This is particularly obvious in MOs 34 and 35 of $ScGe_{16}^-$, MOs 35−37 of $TiGe_{16}$, and MOs 37 and 38 of VGe_{16}^+. Also, the MO 33 does not have either simple p or s character in any of these clusters. We have shown the MO energy diagram and the iso-surface plots for top six occupied MOs for these clusters in Figure S2 in the Supporting Information. Shapes of the top five occupied MOs in these clusters may be compared with the 1d states obtained in TM-alkali clusters.[32] From these, we conclude that there is, indeed, a uniform electron-rich region inside the Ge cage and a filled shell configuration. However, there is no simple one-to-one correspondence between the MOs of these clusters and the states in a spherical free-electron gas.

As $ScGe_{16}^-$ attains enhanced stability due to filled electronic shells, we can expect $ScGe_{16}$ to have a large EA. Indeed, Figure 5a shows that $ScGe_{16}$ has the highest EA among all of the Sc encapsulating clusters. Similarly, as $TiGe_{16}$ is a filled shell cluster, we expect it to have large VDE. This is again borne out by our calculations as shown in Figure 5b. In fact, $TiGe_{16}$ has the highest VDE among Ti encapsulating clusters. Finally, VGe_{16}^+ being a filled shell cluster, we expect VGe_{16} to have a small VDE. This is exactly what we find, as shown in Figure 5b. VDE of the V encapsulating clusters shows a sharp drop from $n = 15$ to 16.

We now focus our attention to the other possible 20-electron clusters. $ScGe_{17}$ and $ScGe_{18}^+$ do have the largest EE among

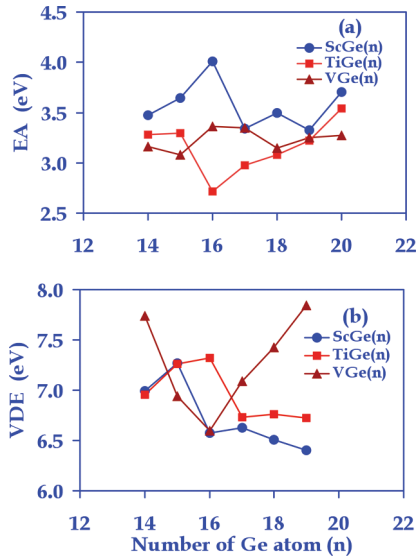

Figure 5. (a) EA and (b) VDE of Sc, Ti, and V encapsulating Ge_n clusters.

the Sc encapsulated neutral and cation clusters, respectively, as seen from Figure 2. However, these clusters do not show peaks in their HOMO−LUMO gaps. One of us has recently shown[32] in the case of TM doped alkali clusters that a peak in alkali addition energy without an accompanying peak in the HOMO−LUMO gap indicates enhanced stability due to geometric features. Therefore, it is natural to assume that these two clusters attain enhanced stability due to their particular geometric structure. This claim is further corroborated by the fact that the Sc atom forms bonds with 13 and 11 Ge atoms, respectively, in $ScGe_{17}$ and $ScGe_{18}^+$ as indicated by the (3, −1) CPs (Figure 1g). Because only the Ge atoms bonded to the TM atom donate electrons to the free-electron gas, these are not 20-electron clusters. The location of the (3, +3) CPs inside the Ge (Figure 1h) cage also shows that there is no uniform electron-rich region, in clear contrast to Figure 1b,d,f. Therefore, although a simple-minded electron count would expect $ScGe_{17}$ and $ScGe_{18}^+$ to be 20-electron filled shell clusters having enhanced stability, our analysis shows that that is not the case.

We next look at the $TiGe_{15}^-$ and $TiGe_{17}^+$ clusters. $TiGe_{15}^-$ shows peaks in EE and the HOMO−LUMO gap. $TiGe_{17}^+$, however, does not show peaks in any of these quantities. If $TiGe_{15}^-$, indeed, is a filled shell cluster, one would expect $TiGe_{15}$ to have a large EA. As can be seen in Figure 5a, $TiGe_{15}$ has a large EA, which drops sharply at $TiGe_{16}$. To find out how many Ge atoms are bonded to the Ti atom and to find visual evidence of the electron gas, we again locate the (3, −1) and (3, +3) CPs inside the Ge_{15} cage as shown in Figure 1i,j. Surprisingly, we find that the Ti atom is bonded to only 13 of the Ge atoms. This leads us to speculate that $TiGe_{15}^-$ is actually an 18-electron cluster showing enhanced stability. However, an electron-rich region is formed only on one side of the Ti atom, unlike in $ScGe_{16}^-$, $TiGe_{16}$, and VGe_{16}^+ clusters. On the other hand, in $TiGe_{17}^+$, the Ti atom is bonded to only 10 Ge atoms leading to a valence electron count of 13. Also, there is no indication of a uniform electron-rich region from the location of the (3, +3) CPs. Finally, among the possible 20-electron clusters, we look at VGe_{15}. This cluster has peaks in EE and HOMO−LUMO gap, indicating its enhanced stability due to a filled shell electronic configuration. If VGe_{15} is a filled shell cluster, the VDE should drop at VGe_{16}. Figure 5b shows that VDE is a minimum for VGe_{16}. Our analysis of the (3, −1) CPs shows that the V atom is bonded to all of the Ge atoms in VGe_{15}, so that the valence electron count around the V atom, indeed, is 20. However, the (3, +3) CPs are located on one side of the V atom, just as in the case of $TiGe_{15}^-$. We have shown the (3, −1) and (3, +3) CPs of $ScGe_{18}^+$, $TiGe_{17}^+$, and VGe_{15} clusters in Figure S1 in the Supporting Information. The absence of formation of a uniform electron-rich region is clear.

Having analyzed the possible 20-electron clusters, we now analyze the stability of the possible 18-electron clusters. The first candidate in the list is $ScGe_{15}$. From Figures 2 and 3, we see that this cluster has peaks in EE and HOMO−LUMO gap, indicating its enhanced stability. To understand if this enhanced stability originates from electronic features, we again locate the (3, −1), and the (3, +3) CPs. As shown in Figure 1k, the Sc atom is bonded to all 15 Ge atoms making the valence electron count on this cluster 18. There are also a large number of (3, +3) CPs located nearly uniformly all around the Sc atom (Figure 1l), indicating formation of a uniform electron-rich region. VDE shows a sharp drop at $ScGe_{16}$ in Figure 5b, indicating a filled shell nature of $ScGe_{15}$. The next candidate in the series is $ScGe_{16}^+$. As is seen from Figures 2 and 3, there is no marked peak, only a plateau in EE. HOMO−LUMO gap also does not have a peak for this cluster. The location of the CPs shows that the Sc is bonded to only 10 Ge atoms, and there is no electron-rich region inside the cage. Therefore, $ScGe_{16}^+$ does not show any enhanced stability. The final candidate that we analyze is $TiGe_{15}^+$. Figures 2 and 3 show that this cluster has peaks in EE and HOMO−LUMO gap. Analysis of CPs reveals that the Ti atom is bonded to 14 of the Ge atoms. This makes the total electron count to be 18, leading to enhancement of stability of this cluster. Moreover, an electron-rich region is seen to form on one side of the Ti atom as in the case of $TiGe_{15}^-$. The (3, −1) and (3, +3) CPs of $ScGe_{16}^+$ and $TiGe_{15}^+$ clusters are also shown in Figure S1 in the Supporting Information.

It deserves a mention that some $TMGe_{18}$ clusters also show peaks in the EEs. In particular, major peaks are observed for $TiGe_{18}$, VGe_{18}, $TiGe_{18}^+$, and VGe_{18}^+ clusters in Figure 2. Minor peaks are seen for $ScGe_{18}^-$, $TiGe_{18}^-$, and VGe_{18}^- clusters. We have already discussed the case of $ScGe_{18}^+$. $ScGe_{18}$, however, has no peak in its EE. From Figure 3, we find that out of these clusters, only $TiGe_{18}^+$ has an appreciable peak in its HOMO−LUMO gap. By our earlier argument, we could claim that except for $TiGe_{18}^+$, enhanced stability of all other clusters at this size originates from geometric effects, while for $TiGe_{18}^+$ it has an electronic origin. However, even in $TiGe_{18}^+$, we do not see any evidence of formation of an electron gas, as seen in Figure S1 in the Supporting Information. Indeed, Figure S1 in the Supporting Information shows that the Ti atom in this cluster is bonded to 11 Ge atoms, giving a valence electron count of 14. There are no indications of electron gas formation in any other cluster at this size either. Therefore, while the exact reason for enhanced stability at this size is unclear, it is not due to electron gas formation in these clusters.

4. Conclusions

These results unravel some of the complexities of the TM encapsulating Ge clusters. (1) These clusters can attain enhanced stability due to electronic or geometric effects. (2) The total number of valence electrons around the TM atom can be known only after analyzing the topology of the MEP. (3) An electron gas is formed only in those clusters that attain stability because of filled shell electronic configurations. These include $ScGe_{16}^-$, $TiGe_{16}$, VGe_{16}^+, and $ScGe_{15}$. (4) Clusters that show enhanced stability having 18 or 20 valence electrons, but have doublet

ground states, have electron gas only on one side of the TM atom inside the Ge cage. These are $TiGe_{15}^-$, $TiGe_{15}^+$, and VGe_{15}. Reasons for this are not clear to us at this time. (5) In other clusters, there is no evidence of an electron gas inside the cage. (6) Many of the clusters having 18 Ge atoms show enhanced stability, but none of these exhibit formation of electron gas inside the Ge cage. We believe this work conclusively shows that one should not attempt to explain all observed stabilities in TM encapsulating semiconductor clusters through simple electron-counting rules.

Acknowledgment. Computations were performed at the cluster computing facility at the Harish-Chandra Research Institute (http://cluster.hri.res.in).

Supporting Information Available: Figure showing enlarged panels for Figure 1 and the CPs for $ScGe_{16}^+$, $ScGe_{18}^+$, $TiGe_{15}^+$, $TiGe_{17}^+$, $TiGe_{18}^+$, and VGe_{15} clusters (Figure S1) and figure showing MO energy plots and iso-surface plots of the top six occupied MOs of $ScGe_{16}^-$, $TiGe_{16}$, and VGe_{16}^+ clusters (Figure S2). This material is available free of charge via the Internet at http://pubs.acs.org.

References and Notes

(1) Hiura, H.; Miyazaki, T.; Kanayama, T. *Phys. Rev. Lett.* **2001**, *86*, 1733.

(2) Khanna, S. N.; Rao, B. K.; Jena, P.; Nayak, S. K. *Chem. Phys. Lett.* **2003**, *373*, 433.

(3) Ma, L.; Zhao, J. J.; Wang, J. G.; Wang, B. L.; Lu, Q. L.; Wang, G. H. *Phys. Rev. B* **2006**, *73*, 125439.

(4) Mprourmparkis, G.; Froudakis, G. E.; Andriotis, A. N.; Menon, M. *J. Chem. Phys.* **2003**, *119*, 7498.

(5) Ohara, M.; Miyajima, K.; Pramann, A.; Nakajima, A.; Kaya, K. *J. Phys. Chem. A* **2002**, *106*, 3702.

(6) Ohara, M.; Koyasu, K.; Nakajima, A.; Kaya, K. *Chem. Phys. Lett.* **2003**, *371*, 490.

(7) Koyasu, K.; Akutsu, M.; Mitsui, M.; Nakajima, A. *J. Am. Chem. Soc.* **2005**, *127*, 4998.

(8) Jaeger, J. B.; Jaeger, T. D.; Duncan, M. A. *J. Phys. Chem. A* **2006**, *110*, 9310.

(9) Guo, L.-J.; Zhao, G.-F.; Gu, Y.-Z.; Liu, X.; Zeng, Z. *Phys. Rev. B* **2008**, *77*, 195417.

(10) Koyasu, K.; Atobe, J.; Akutsu, M.; Mitsui, M.; Nakajima, A. *J. Phys. Chem. A* **2007**, *111*, 42.

(11) Andriotis, A. N.; Mpourmpakis, G.; Froudakis, G. E.; Menon, M. *New J. Phys.* **2002**, *4*, 78.

(12) Wang, J.; Ma, Q.-M.; Xie, Z.; Liu, Y.; Li, Y.-C. *Phys. Rev. B* **2007**, *76*, 035406.

(13) Kawazoe, Y.; Kumar, V. *Phys. Rev. Lett.* **2001**, *87*, 045503.

(14) Khanna, S. N.; Rao, B. K.; Jena, P. *Phys. Rev. Lett.* **2002**, *89*, 016803.

(15) Kawazoe, Y.; Kumar, V. *Phys. Rev. Lett.* **2003**, *90*, 055502.

(16) Nagase, S.; Lu, J. *Phys. Rev. Lett.* **2003**, *90*, 115506.

(17) Sen, P.; Mitas, L. *Phys. Rev. B* **2003**, *68*, 155404.

(18) Reveles, J. U.; Khanna, S. N. *Phys. Rev. B* **2005**, *72*, 16513.

(19) Reveles, J. U.; Khanan, S. N. *Phys. Rev. B* **2006**, *74*, 035435.

(20) Wigner, E.; Witmer, E. E. *Z. Phys.* **1928**, *51*, 859.

(21) de Heer, W. A. *Rev. Mod. Phys.* **1993**, *65*, 611.

(22) Kawazoe, Y.; Kumar, V. *Phys. Rev. Lett.* **2002**, *88*, 235504.

(23) Wang, J.; Han, J.-G. *J. Phys. Chem. B* **2006**, *110*, 7820.

(24) Bandyopadhyay, D.; Sen, P. *J. Phys. Chem. A* **2010**, *114*, 1835.

(25) Bader, R. F. W. *Atoms in Molecules, A Quantum Theory*; International Monographs on Chemistry ; Clarendon Press: Oxford, 1990; Vol. 22.

(26) Leboeuf, M.; Köster, A. M.; Jung, K.; Salahub, D. *J. Chem. Phys.* **1999**, *111*, 4893, and refernces therein.

(27) Becke, A. D. *J. Chem. Phys.* **1993**, *98*, 5648.

(28) Perdew, J. P.; Yang, Y. *Phys. Rev. B* **1992**, *45*, 13244.

(29) Frisch, M. J.; Trucks, G. W.; Schlegel, H. B.; Scuseria, G. E.; Robb, M. A.; Cheeseman, J. R.; Montgomery, J. A., Jr.; Vreven, T.; Kudin, K. N.; Burant, J. C.; Millam, J. M.; Iyengar, S. S.; Tomasi, J.; Barone, V.; Mennucci, B.; Cossi, M.; Scalmani, G.; Rega, N.; Petersson, G. A.; Nakatsuji, H.; Hada, M.; Ehara, M.; Toyota, K.; Fukuda, R.; Hasegawa, J.; Ishida, M.; Nakajima, T.; Honda, Y.; Kitao, O.; Nakai, H.; Klene, M.; Li, X.; Knox, J. E.; Hratchian, H. P.; Cross, J. B.; Bakken, V.; Adamo, C.; Jaramillo, J.; Gomperts, R.; Stratmann, R. E.; Yazyev, O.; Austin, A. J.; Cammi, R.; Pomelli, C.; Ochterski, J. W.; Ayala, P. Y.; Morokuma, K.; Voth, G. A.; Salvador, P.; Dannenberg, J. J.; Zakrzewski, V. G.; Dapprich, S.; Daniels, A. D.; Strain, M. C.; Farkas, O.; Malick, D. K.; Rabuck, A. D.; Raghavachari, K.; Foresman, J. B.; Ortiz, J. V.; Cui, Q.; Baboul, A. G.; Clifford, S.; Cioslowski, J.; Stefanov, B. B.; Liu, G.; Liashenko, A.; Piskorz, P.; Komaromi, I.; Martin, R. L.; Fox, D. J.; Keith, T.; Al-Laham, M. A.; Peng, C. Y.; Nanayakkara, A.; Challacombe, M.; Gill, P. M. W.; Johnson, B.; Chen, W.; Wong, M. W.; Gonzalez, C.; Pople, J. A. *Gaussian 03*, revision D.1; Gaussian, Inc.: Wallingford, CT, 2003.

(30) Köster, A. M.; et al. *deMon2K* V 2.3.6; International deMon Developers' Community: Cinvestav, Mexico, 2007. Available at http://www.deMon-software.com.

(31) Bandyopadhyay, D. *J. Appl. Phys.* **2008**, *104*, 084308.

(32) Reveles, J. U.; Sen, P.; Pradhan, K.; Roy, D. R.; Khanna, S. N. *J. Phys. Chem. C* **2010**, *114*, 10739.

JP106354D